SUPPORTING INFORMATION for the paper:

Structural diversity and energetics of anhydrous lithium tartrates: experimental and computational studies of novel chiral polymorphs and their racemic and meso analogues.

Hamish H.-M. Yeung†, Monica Kosa‡, Michele Parrinello‡, Paul M. Forster§, and Anthony K. Cheetham†*

† Department of Materials Science and Metallurgy, University of Cambridge, Pembroke Street, Cambridge, U.K., CB2 3QZ. ‡ Department of Chemistry and Applied Biosciences, ETH Zurich, USI-Campus, Via G. Buffi 13, 6900 Lugano, Switzerland. § Department of Chemistry, University of Nevada, Las Vegas, 4505 South Maryland Parkway, Box 454003, Las Vegas, NV 89154-4003, U.S.A.

*To whom correspondence should be addressed. E-mail: akc30@cam.ac.uk. Fax: +44 1223 334567

Supporting Information 1. Simulataneous differential scanning calorimetry (dotted purple) and thermogravimetric analysis (red) (SDT) of Li_2(L-tartrate), **2**, Li_2(L-tartrate), **3** and Li_2(D,L-tartrate), **5**.

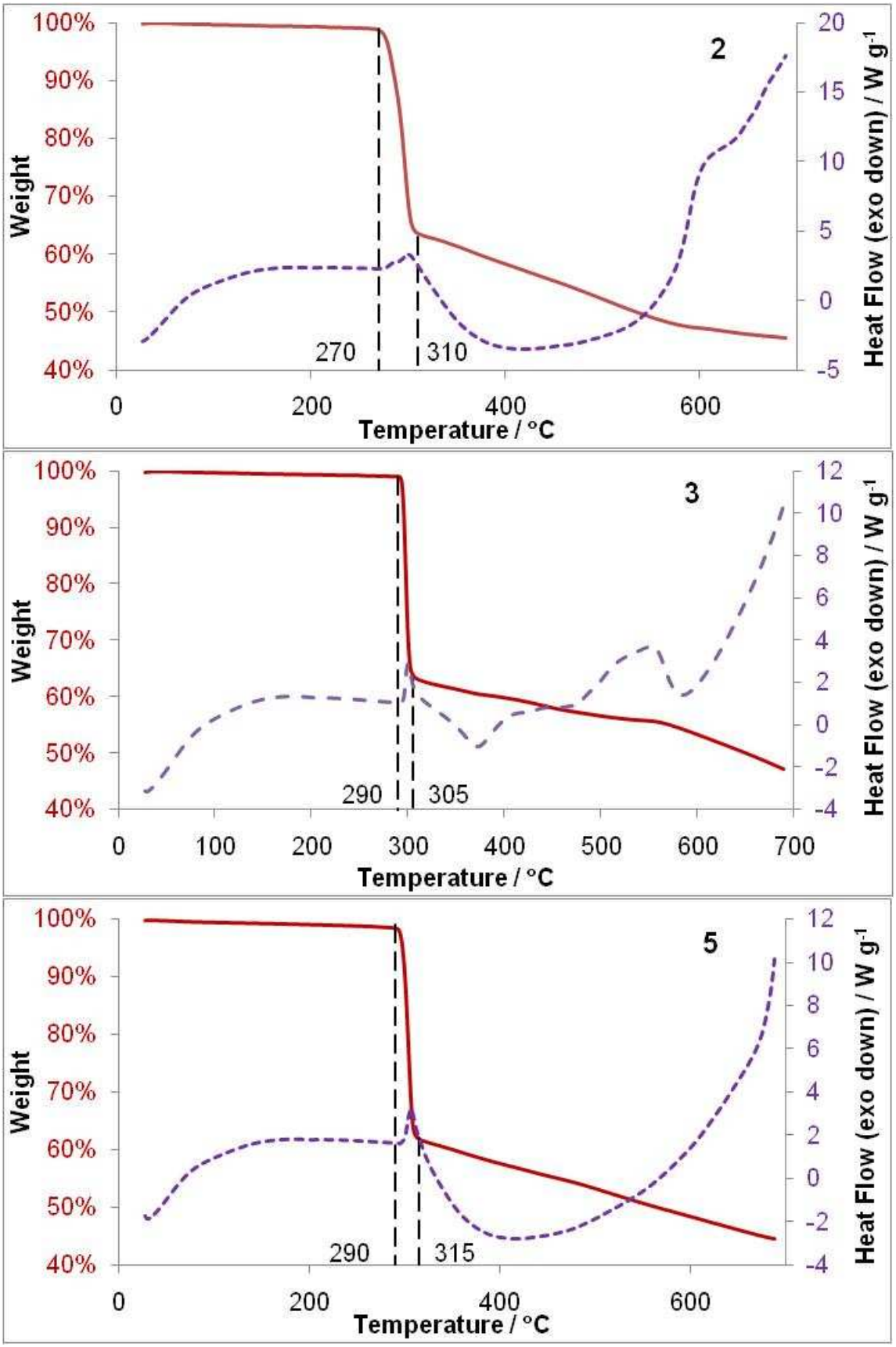

Supporting Information 2. Simulataneous differential scanning calorimetry (dotted purple line) and thermogravimetric analysis (solid red line) (SDT) of the impure source reaction of LiH(L-tartrate), **1**, showing loss of coordinated small molecules (likely to be solvent, ethanol of THF, or water from hydrated precursors) at 130 – 145 °C (5 %), decomposition of an unknown anhydrous phase at 250 – 300 °C (15 %), and further decomposition from 350 °C. The initial loss at 135 – 145 °C is smaller than would be expected from a single hydrated lithium tartrate phase ($Li_2(C_4H_4O_6)\cdot H_2O$ FW 180 g mol^{-1}; H_2O FW 18 g mol^{-1}, 10 %).

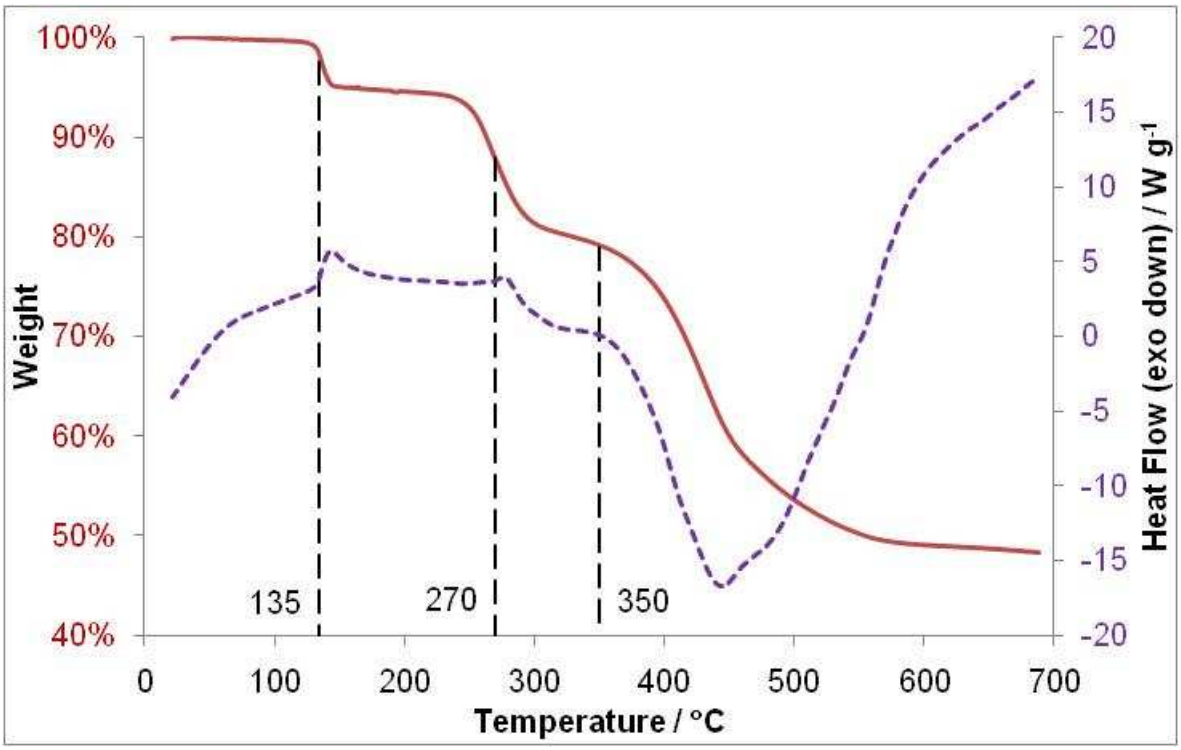

Supporting Information 3. Simulataneous differential scanning calorimetry (dotted purple line) and thermogravimetric analysis (solid red line) (SDT) of the impure source reaction of Li_2(*meso*-tartrate), **4**. Inset shows main region of decomposition, expanded in the temperature axis to show clearly the two steps corresponding to different anhydrous phases.

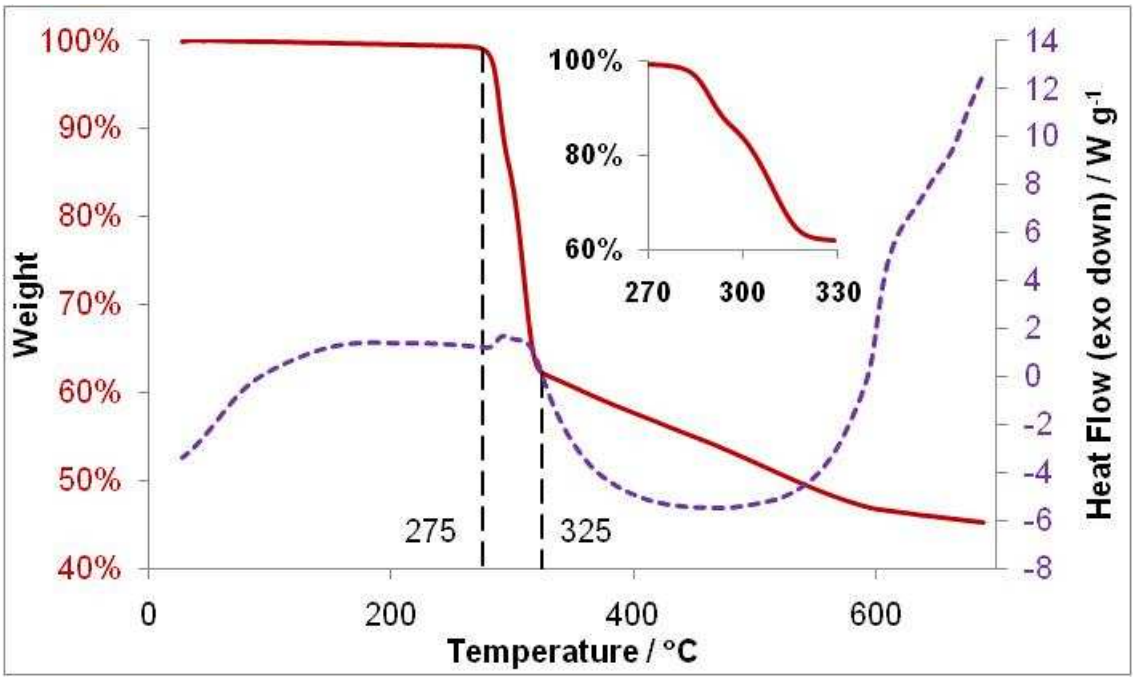

Supporting Information 4. Simulated (red dotted lines) and observed (blue solid lines) powder X-ray diffraction patterns for dilithium L-tartrates **2** and **3** and dilithium D,L-tartrate **5**.

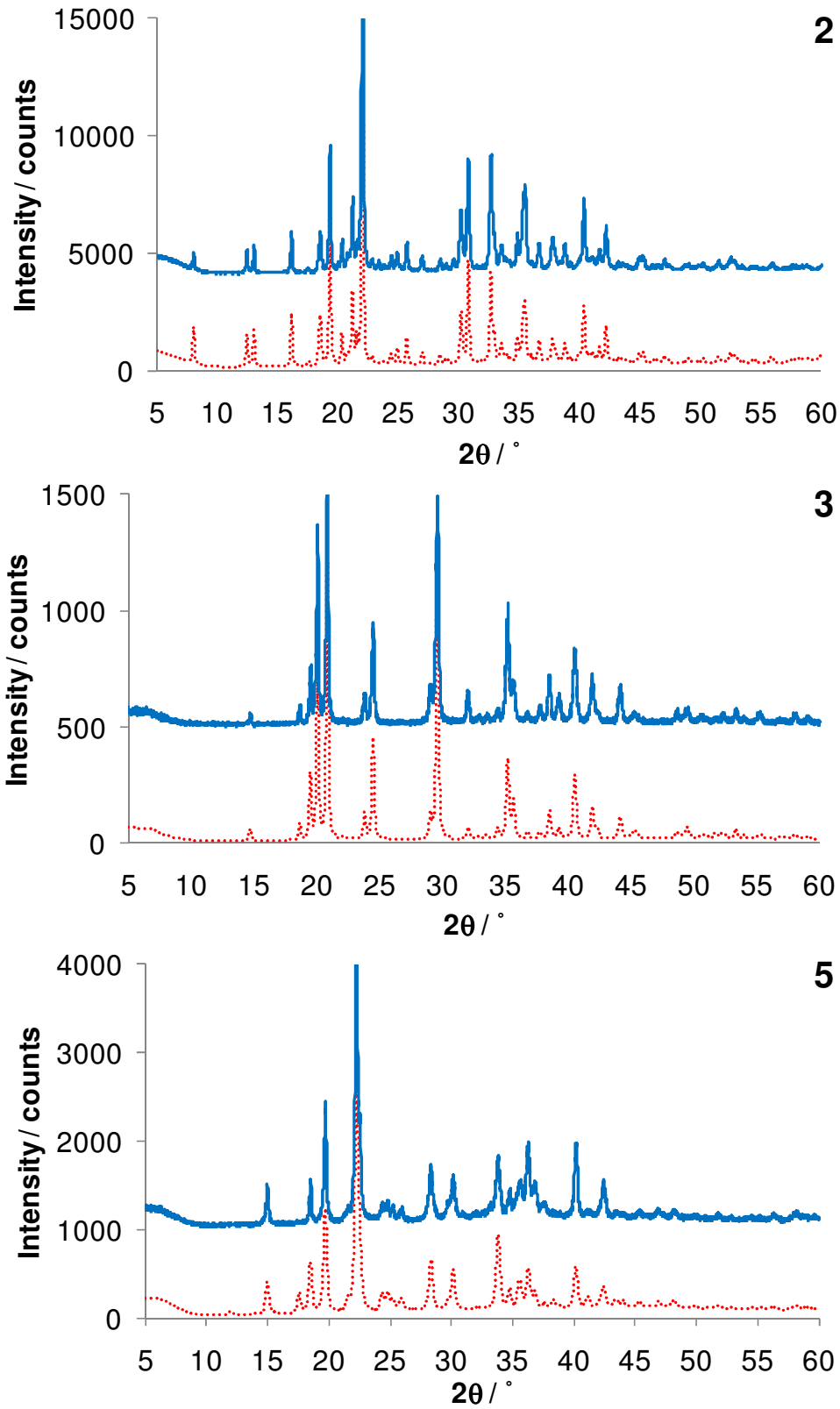

Supporting Information 5. Powder X-ray diffraction pattern of impure source reaction of **4** (solid blue line) and simulated pattern of Li_2(*meso*-tartrate), (monoclinic $P2_1/c$, cell parameters a = 6.471(2) Å, b = 5.014(2) Å, c = 9.028(4) Å, β = 95.83(3)°, dotted red line), discovered subsequent to initial submission of the manuscript. Crosses show those peaks not explained by the simulated pattern.

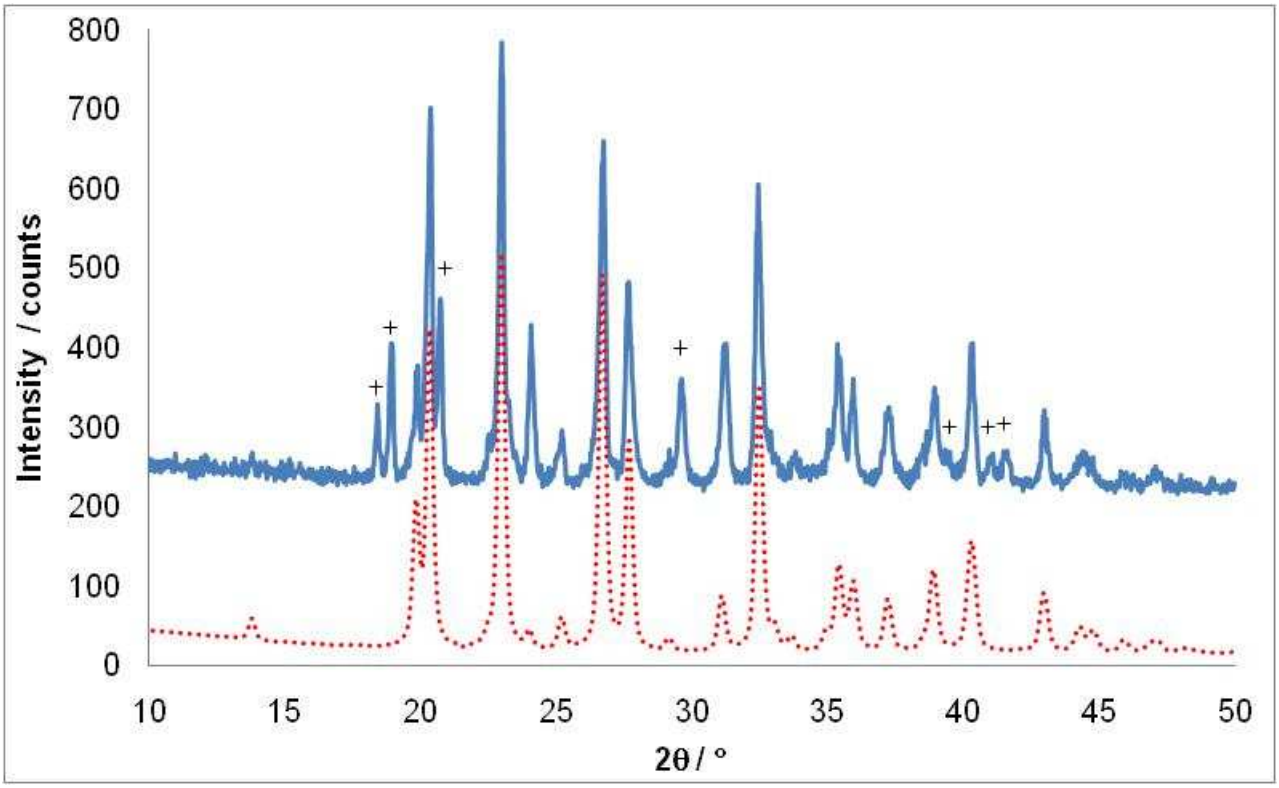

Supporting Information 6. Total energy plotted as a function of plane wave density cutoff for relative cutoff 50 Ry (solid blue diamonds) and 40 Ry (open red squares).

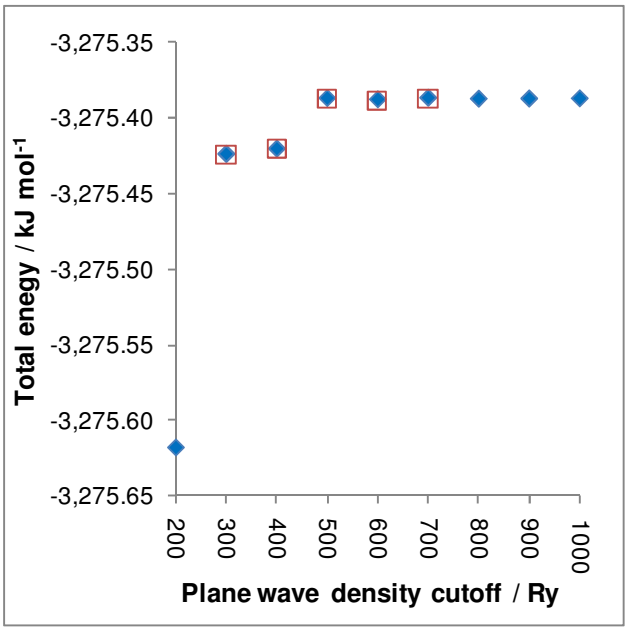

Supporting Information 7. Absolute and relative calculated values of the total energy, E_{elec}, zero point vibrational energy, ZPVE, and thermal contribution to the vibrational energy at 295.15 K, E_{vib}, of dilithium tartrates **2** – **5**.[a]

	2	**3**	**4**	**5**
Empirical formula	Li_2(L-tart)	Li_2(L-tart)	Li_2(*meso*-tart)	Li_2(D,L-tart)
Space group	$P2_12_12_1$	$C222_1$	$P2_1/c$	$C2/c$
Total electronic energy, E_{elec} / kJ mol^{-1}	-358315.95	-358319.80	-358317.97	-358315.27
Zero point vibrational energy, ZPVE / kJ mol^{-1}	280.28	264.91	264.59	266.16
Thermal contribution, E_{vib} / kJ mol^{-1}	18.59	23.44	23.97	24.22
Relative electronic energy, ΔE_{elec} / kJ mol^{-1}	**3.85**	**0.00**	**1.83**	**4.53**
Relative zero point vibrational energy, ΔZPVE / kJ mol^{-1}	15.37	0.00	-0.32	1.25
Relative thermal contribution, ΔE_{vib} / kJ mol^{-1}	-4.85	0.00	0.53	0.78
Δ(E+ZPVE) / kJ mol^{-1}	19.22	0.00	1.51	5.78
Δ(E+ZPVE+E_{vib}) / kJ mol^{-1}	**14.37**	**0.00**	**2.04**	**6.56**

[a]all values are normalised to one mole of formula unit.

Supporting Information 8. Plot of calculated normal mode frequencies for $Li_2(L\text{-}C_4H_4O_6)$, **2**, (blue diamonds) and $Li_2(L\text{-}C_4H_4O_6)$, **3**, (red squares). Inset shows first 600 normal modes expanded horizontally, for clearer comparison of the low frequency (heavy atom) region.

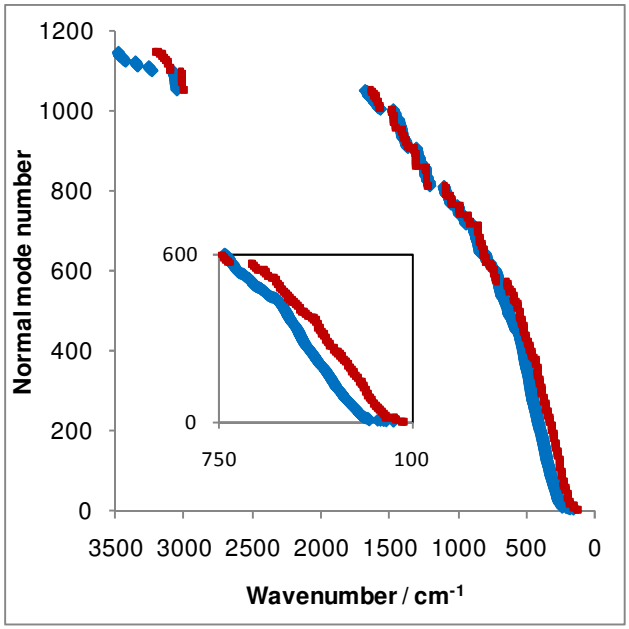

Supporting Information 9. Table from Appelhans *et al.*,[1] updated to include $\Delta(E_{elec}+ZPVE)$ and $\Delta(E_{elec}+ZPVE+E_{vib})$.

Phase	ΔE_{elec} / kJ mol^{-1}	$\Delta(E_{elec}+ZPVE)$ / kJ mol^{-1}	$\Delta(E_{elec}+ZPVE+E_{vib})$ / kJ mol^{-1}	Calorimetry / kJ mol^{-1}
Ca(*meso*-$C_4H_4O_6$)	0	0	0.0	0
Ca(L-$C_4H_4O_6$)	9.1	8.0	7.7	2.9 ± 1.6
Sr(*meso*-$C_4H_4O_6$)	0	0	0.0	0
Sr(L-$C_4H_4O_6$)	13.4	11.0	11.5	8.1 ± 1.4
Ba(L-$C_4H_4O_6$)	0	0	0.0	0
Ba(D,L-$C_4H_4O_6$)	6.4	4.5	5.6	7.0 ± 1.0

(1) Appelhans, L. N.; Kosa, M.; Radha, A. V.; Simoncic, P.; Navrotsky, A.; Parrinello, M.; Cheetham, A. K. *J. Am. Chem. Soc.* **2009,** *131*, (42), 15375-15386.